Low price Fuel Cell Inverter System for 3[KW] Residential Power

Soon-Kurl Kwon*

Abstract

This study proposed a high efficiency DC-DC converter with a new current doubler rectifier for fuel-cell systems for use with the Nexa(310-0027) PEMFC from the Ballard Co. The proposed high efficiency DC-DC converter for the fuel-cell system generated ZVS by applying partial resonance and using a phase shift PWM control method. Constantly switching frequency, loss of switching, peak current, and peak voltage were reduced by this system. In addition to this system, two inductors were attached to a rectifier circuit allowing it to be able to provide the direct current(DC) and DC voltage safely to a load with reduced ripple components. Also, by using the newly proposed current doubler rectifier, the high frequency DC-DC converter for the fuel cell system was capable of reaching a highest efficiency of 92[%] as compared to 88.3[%] efficiency in previous results, which means that efficiency increased 3.7[%]. The overall results were confirmed by a simulation and laboratory experiment.

Key Words : Current Doubler Rectifier, Phase Shift, DC-DC Converter for Fuel Cell System

1. Introduction

Generally, an electric-power converter, which is used for fuel-cell generation systems, plays a role in converting the output of DC from the body of a fuel-cell machine into the amount of voltage and frequency of alternating current(AC) needed by the user. Also, the power of the low voltage must be boosted and the output of the voltage generated to a fixed voltage. Since the stack of the fuel cell

* Main author : Department of Electrical
         Engineering, Kyungnam University
 Tel : +82-55-249-2633 Fax : +82-55-242-2683
 E-mail : soonkurl@kyungnam.ac.kr
 Date of submit : 2007. 1. 26
 First assessment : 2007. 1. 29
 Completion of assessment : 2007. 2. 12

outputs DC approximately to 22~48[VDC], an electric-power converter, which converts to 60[Hz] in alternation, is needed after boosting the voltage to 400[VDC]. Also, the particular features of the fuel-cell do not allow it the ability to store energy. This is why a fuel-cell has the structure of a multi-electric-generator system with the addition of an energy-storage installation such as a battery or super-catheter in order to contribute to the ability to respond rapidly when the system must start or when there are extreme load changes [1-8]. The output of the fuel-cell has its own features of low voltage and a high current that changes its voltage based on its load. It is necessary to reduce this voltage because of ᵗ͟ᵉ

high ripple of the current, which originates from the fuel-cell system [9-12]. In this experiment, in order to solve problems stated above, a new high frequency DC-DC converter for a fuel-cell system is proposed by applying a current doubler rectifier. After the proposed high frequency DC-DC converter of the fuel-cell system attaches two inductors to a previously used insulating full-bridge converter, the second side of the transformer current must be decreased to half of the current that originates from the load side. This is the way the current doubler rectifier operates, which has the unique feature of reducing the ripple of the output of the current. Also, by using the phase shift PWM control method, by controlling the fixed frequency, and by attaining a zero-voltage switching, loss of the switching was lessened. These results were confirmed through laboratory experiment and simulations.
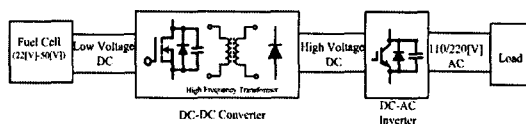
2. Topology of the Electric-Power Converter for the Fuel-Cell Generation System

According to the voltage output of the fuel-cell, the capacity, applied field, or various forms, the topology of the electric-power converter for the fuel-cell is divided into two different parts(See Figs. 1 and 2). Fig. 1 shows two different techniques that make the voltage of the fuel-cell boost when the electric power is converted in order to receive the fuel-cell generation. Fig. 1 (a) primarily converts the low voltage of the fuel-cell into a low AC by applying a DC-AC inverter. After that, upon using a low frequency(60[Hz]) transformer, a relatively high efficiency can result through an electric-power conversion method, which insulates and boosts the voltage. On the other hand, because a low-frequency transformer is used, its weight(10[kg/kW]) and volume are

increased, and, because it is not feasible to regulate the DC voltage, this has the disadvantage of causing the quality of the voltage output to decline. Fig. 1 (b) outlines a series of steps: (1) the low voltage of the fuel cell, (2) a DC-DC converter using a high-frequency transformer, (3) a high DC-link voltage(400[V]), (4) a DC-AC inverter after boosting and regulating the voltage, (5) the AC, which is necessary for the load. At this point, the high-frequency transformer that is used in the DC-DC converter is low in volume and weight, so it is possible to miniaturize the total transformer. Further, the voltage output has great quality since the DC-link voltage is controlled. However, it is difficult to gain high efficiency from it because it must pass through two different stages in the electric-power converter. Supposedly, the efficiency of the DC-DC converter is 92[%] while the DC-AC inverter is 96[%] efficient, but the efficiency of the total electric-power converter is only 88.3[%]. If the voltage of the fuel-cell is low, in particular, it is even more difficult to gain high efficiency from the DC-DC converter. Hence, research to promote the efficiency of the converter is in progress [1-4].
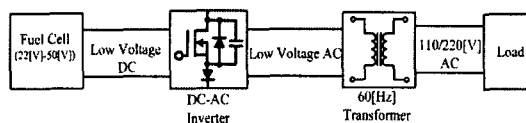
(a) Boost method for AC-AC voltage by using a low-frequency transformer

(b) Boost method for DC-DC voltage by using a high-frequency transformer

Fig. 1. Boost methods

Fig. 2 generally indicates both the advantages and disadvantages of electric-power converters, which are used for the electric generator system of the fuel cell.
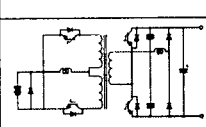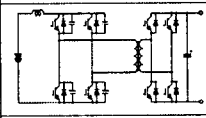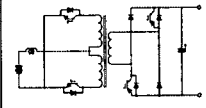

Fig. 2. Conventional fuel-cell generation system power conversion system

According to Fig. 2, it is very difficult for the converter of a non-insulating method to receive a high boost in voltage, so an insulating method using a high-frequency transformer is usually utilized. Topology with a low core usage was not considered. Because the current that was flowing throughout the system cannot make an immediate change in its directions when the insulating full-bridge converter switches off, there will be an extreme voltage change originating from the leakage inductor. This immediate boost in the voltage may damage the device, create a loss of switching from the high-frequency operation, and may produce a serious noise. In order to solve these problems, an RCD snubber circuit, which is composed of resistance and a capacitor, is used, but the disadvantage in this is an inappropriate application to a large amount of electric-power [4-7]. Therefore, in this study, a new DC-DC converter for a fuel-cell generation system is proposed by using a current doubler rectifier method(See Fig. 3).

3. The Proposed Electric-Power Converter for Fuel-Cells

3.1 A Modeling of the Fuel-Cell

Fig. 3 is a Pspice modeling circuit of a fuel-cell. In this figure, it can be seen that a diode moves in the domain of the activation polarization, two BJTs are used to remodel the domain of the concentration polarization, and an ohmic polarization is remodeled by the parasitic resistance of the diode. If the diode that is used for the activation polarization is carefully observed, the diode that is built by the p-n junction forms a potential barrier with the depletion layer. The voltage of the diode can be described as an equation (1), and it is similar to an activation overvoltage.

$$V_{diode} = nV_{Th} \times \ln\frac{i_D}{i_s}, \qquad V_{Th} = \frac{kT}{q} \qquad (1)$$

Where, n: divergence factor, V_{TH}: heat voltage, i_s: saturation current, ip: diode current, k: Boltzmann constant, T: temperature in Kelvin, q: electric charge, V_{diode}: voltage on both sides of the diode.
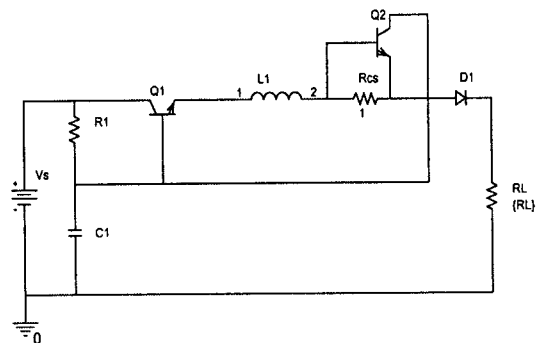

Fig. 3. Pspice modeling circuit of a fuel cell

Upon choosing a parameter from the Pspice, the diode, which is equivalent to the feature of voltage-current for the fuel-cell, can be remodeled. The diode parameters that are used for the remodeling are Is(Saturation current), Rs(Parasitic resistance), and N(Emission Coefficient). In that order, they are assigned to be: I_s=0.02[A], R_s=0.1[O], and N=80. The ohmic polarization is remodeled by using the parasitic resistance of the diode. The concentration polarization is remodeled by using a current limit circuit. As Fig. 4 indicates, the current limit circuit is composed of BJT Q_1 and Q_2, and current-sensing resistance, R_{cs}. If an over-current flows through the R_{cs}, the Q_2 becomes conversant, and the base voltage of the Q_1 is decreased. By the theory, an emitter voltage of the Q_1 becomes reduced exponentially as in the equation, which allows the concentration polarization to emerge. The capacitor C_1 is connected in parallel by an interfacial bilayer of the electrode and electrolyte. Due to the component of the capacitor, the voltage changes slowly as the current changes instantly. In addition, an inductor L_1 is a remodeled air compressor for the fuel-cell system. For Ballard's Nexa(310-0027) PEMFC model, which was used in this study, a circuit parameter is applied. The circuit parameter is V_s=43[V], R_1=0.29[Ω], L_1=10[mH], C_1=1F, R_{cs}=1 [Ω]. Fig. 4 compares the experimental data to the V-I curve of the Pspice modeling circuit by
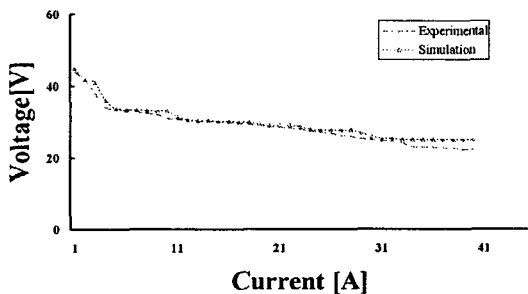

Fig. 4. Simulation and experimental V-I characteristics curve

utilizing Ballard's Nexa PEMFC. According to the comparison, the two features are almost equivalent to each other.

3.2 The Design of the DC-DC Converter for Fuel-Cells

Fig. 5 demonstrates the proposed high-efficiency DC-DC converter for a fuel-cell system. The proposed electric-power converter is composed of the full-bridge, which means that a ZVS lossless capacitor is connected in parallel to each switch of the electric-power semiconductor. Every switch turns on during a half period(including nature time) in an intersectional(S_2-S_3, S_1-S_4) manner.
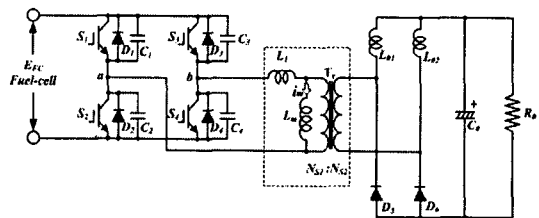

Fig. 5. Composition of proposed fuel-cell generation system.

A phase-shift PWM control method was used to receive the electric-power output with a control signal by using the difference between turning on Switch S_1 and turning on Switch S_4. Upon using this control method, the ZVS is accomplished by a partial resonance, and a constant switching frequency, a loss of switching, and peak voltage and current are reduced. Furthermore, a high-frequency transformer has regard for a leakage inductance(L_l), a magnetization inductance (L_m), and a ratio of the number of volumes (n(=N_s/N_p)). The transformer is composed of a reversed L-shape equivalent circuit. The voltage and current that are transferred by the high-frequency transformer use two output inductors for the current doubler rectifier method

and are composed of a system that provides a leveled DC voltage and current to the load.

3.2.1 An Alternative to MOSFET

Fig. 6 generally demonstrates a waveform of the voltage and current when the switch turns on and off during a given period. When the switch turns on and off, the switch loss is composed of two different losses: a loss from reiteration between the voltage and current and a loss from an attainable electric resistance. In particular, there are many losses originating from the attainable electric resistance of the switch due to the large current feature of the fuel-cell. It is necessary to use Equations 2 and 3 in choosing a device which has a low attainable electric resistance.

$$P_T = P_{ON} + P_S + P_{OFF} \qquad (2)$$

$$P_S = P_{SON} + P_{SOFF} \qquad (3)$$

Where, P_T: total loss, P_{ON}: attainable electric loss, P_{OFF}: interception loss, P_s: switching loss, P_{SOFF}: switching loss when turned off, P_{SON}: switching loss when turned on
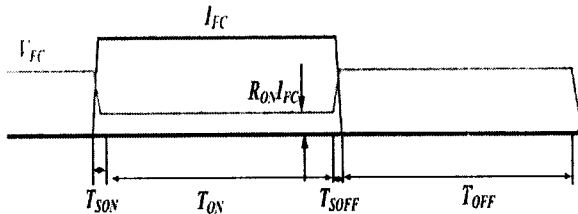

Fig. 6. One cycle switching waveforms

In this study, the practical elements of the switch such as a surge voltage and current were considered and MOSFET FQP65N06(65[A], 60[V], R_{on}=16[mΩ]) from Fairchild Semiconductor Co. was used because this apparatus had a higher level than the one that was designed.

3.2.2 Design of the High-Frequency Transformer

A high-frequency transformer is required to boost the low voltage of the fuel-cell. Hence, through the research process, by using the current doubler rectifier method, the load current was doubled after the load voltage output was made at half the voltage of the second side of the transformation. This study used 1[kW] as the standard level, 380[V] and 3[A] as the output, and a PC40 from TDK Co. as the quality of the core. The following were also used in this study: B_{SAT}=0.45T for saturation magnetic-flux density, $\triangle B$=0.2T for magnetic-flux density, and D_{MAX}= 0.4 for maximum duty ratio. In general, in order to determine the size of the core, the core must convert the first side of energy into the second side of energy without being saturated by the magnetic-flux. The equation for generating the maximum amount of energy is as follows.

$$P_o = I_0 \cdot (V_0 + V_{DF}) = 3(380 + 1) = 1143[VA] \qquad (4)$$

Where, P_o: total electric-power output, I_0: current output, V_0: voltage output, V_{DF}: falling of the total voltage directions of the diode.

The equation of the sum of the electric-power core is as follows.

$$\left. \begin{aligned} \Sigma VA &= \sqrt{\frac{1 + D_{max}}{D_{max}}} + \sqrt{\frac{2}{n}} \times P_0 \\ &= \sqrt{\frac{1 + 0.4}{0.4}} + \frac{\sqrt{2}}{0.95} \times 1143 \\ &= 2553[VA] \end{aligned} \right\} \qquad (5)$$

After the sum(ΣVA) of the electric-power core is generated, the multiplication(A_p) of an effective sectional area and window area must be substituted in the equation.

$$A_p = A_w \cdot A_e$$

$$A_p = (\frac{\Sigma VA \times 10^4}{K_\Delta BK_uK_f\sqrt{\Delta T}})^{1.14} = 17.26[cm^4]$$

$$\Delta T = 40$$

$$K_u = 0.4, \quad K_f = 50, \quad K = 4.88$$

$$\Delta B = 0.20[T]$$

$$(6)$$

Therefore, the PC40-EC90 from TDK Co. was chosen as the core for this study, and the size of the sectional area(A_w) and window area(A_e) is described below.

$$A_e = 626[mm^2], \quad A_w = 1420[mm^2] \tag{7}$$

Equation 8 shows how to obtain the winding wire ratio of the transformer.

$$D = \frac{1 \cdot N_s \cdot V_{in}}{2 \cdot N_p \cdot V_{out}} \tag{8}$$

If the DC-link voltage is set as 380[V], the lowest voltage of the fuel-cell becomes 22[V]. When the highest duty ratio is 0.45 with regard for the turn-off time, the winding wire ratio of the high-frequency transformation becomes N_p: N_s=1:15.5. However, through the research, it was decided that is was 1:16 for the duty loss by leakage inductance of the high-frequency transformation.

3.2.3 Selection of the Diode Rectification or Filter

In general, if the highest voltage through the diode rectification is 400[V] and the highest current is 3[A], a higher level apparatus should be selected with regard for the surge voltage and current than the one that was designed before. Therefore, DSEI20(1200[V] and 17[A]) from IXYS Co. was selected for this study. At this point, the size of the inductor and capacitor can be described

as in Equations 9 and 10.

$$L = \frac{V_o(0.5 - D_{min})}{2\Delta I_{o(min)}f_s}$$

$$= \frac{380(0.5 - 0.2)}{2 \times 0.5 \times 40 \times 10^3}$$

$$= 2.8[mH]$$

$$(9)$$

$$C = \frac{V_o(0.5 - D_{min})}{8L\Delta V_o f_s^2}$$

$$= \frac{380 \times (0.5 - 0.2)}{8 \times 2.8 \times 10^{-3} \times 3.8 \times (40 \times 10^3)^2}$$

$$= 3.2[uF]$$

$$(10)$$

The size of the capacitor calculated by Equation 10 was 3.2[uF]. However, in order to store enough energy in the case of a load change, a capacitor with 2200[uF] was selected for this experiment.

3.3 An Operation Theory of the DC-DC Converter for Fuel-Cells

Fig. 7 demonstrates each voltage and current operation waveform of the DC-DC converter for the fuel-cell system. An operation waveform for a period, including a gate signal, is also indicated.
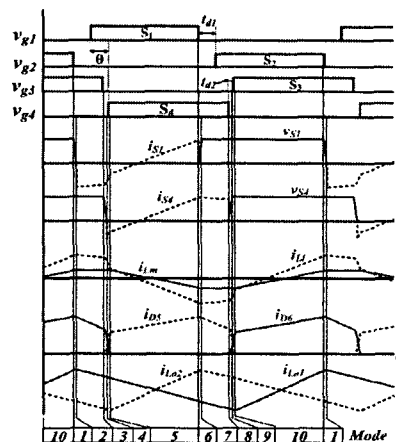

Fig. 7. The voltage and current operation waveforms of the DC-DC converter

Fig. 8 demonstrates the mode equivalent circuit of the proposed high-efficiency DC-DC converter for fuel-cell systems. In order to explain the operation theory, the Switches S_2 and S_3 must be on, and it is hypothesized that after Mode 10,

(a) Mode 1

(b) Mode 2

(c) Mode 3

(d) Mode 4

(e) Mode 5

Fig. 8. Equivalent circuit during a half period of the DC-DC converter

which provides the electric-power to the load, it is reactivated.

Mode 1: ZVS Reflux Period of a Preceding Phase

Mode 1 is the mode that turns off Switch S_2 after Mode 10. At this point, due to the inverter current output, Capacitor C_1 is discharged, and C_2 is charged.

During this period, assuming a constant inverter current output, the equation for the voltage through Switch S_2 is as follows.

$$V_{(S_2)} = \frac{1}{2C}(i_{L_m}(t_0) + n \times i_2(t_0))t \tag{11}$$

Where, C: lossless capacitor, $i_{Lm}(t_0)$: magnetization current at t_0, n: a ratio of a number of volumes on transformer(N_s/N_p), $i_2(t_0)$: the second current side of the transformer at t_0, t: time

When this voltage equation becomes $C_1 = 0$ and $C_2 = EFC$, it moves to the next mode. The dead-time of the preceding phase must be designed with a longer time than the charged / discharged time of C_1 and C_2.

Mode 2: Current Reflux Period(t_1-t_2)

In Mode 2, the current that was flowing through Capacitor C_1 now flows through Diode D_1 and eventually turns to the current reflux mode after the preceding phase of the switch has completed its conversion. At this point, when Diode D_1 is electrically attained, Switch S_1 turns on to ZVS and ZCS. During this period, in order for the transformer to reach the ZVS and ZCS, the current circulation flows. The current circulation also flows for the level at the current doubler rectifier part.

Mode 3: Current Reflux Period(t_2-t_3)
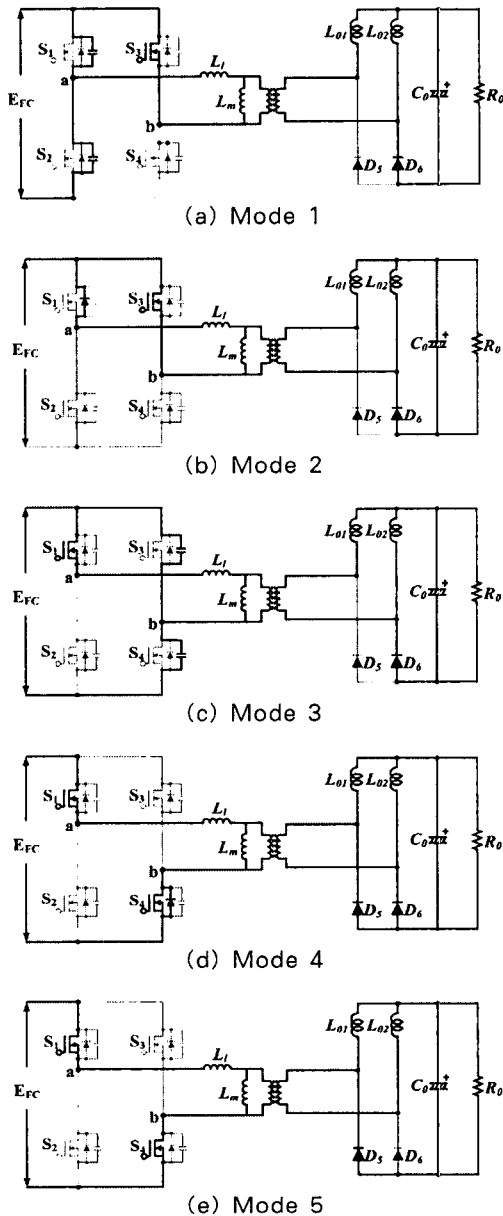
During the reflux period, Switch S_3 is turned off

and is transferred to ZVS in Mode 3. At this point, due to the inverter current output, Capacitor C₃ is charged, and C₄ is discharged. Since the current side of the transformer becomes 0[V] in Mode 3, it can be considered a short circuit. Hence, the voltage through Switch S₃ or the inverter current output is demonstrated by Equations 12 and 13.

$$V_{(s_3)} = \sqrt{\frac{L_1}{2C}}\,(i_{L_m}(t_2)+n\times i_2(t_2))\sin\frac{t}{\sqrt{2CL_1}} \qquad (12)$$

$$i_{(inv.)} = (i_{L_m}(t_2)+n\times i_2(t_2))\cos\frac{t}{\sqrt{2CL_1}} \qquad (13)$$

Where, iLm(t₂): magnetization current at t₂, I₂: the second current side of the transformer at t₂, L₁: leakage inductance

Capacitor C₃ is charged by Equations 12 and 13, Capacitor C₄ is discharged, and Switch S₄ is turned on to ZVS.

Mode 4: The Current Doubler Rectifier Period
(t₃–t₄)

In this mode, Capacitors C₃ and C₄ are charged / discharged. At this point, the current that flows through C₄ is converted into Diode D₄. After this, when D₄ is in an attainable electric state, Switch S₄ is turned on to ZVS and ZCS.

Mode 5: The Current Supply Period(t₄–t₅)

After the energy that was in Diode D₆ is converted into Diode D₅, the current from the power is supplied to the load. During this period, a voluntary voltage output can be obtained if the duty ratio is adequately adjusted.

Overall, the operation theory that was related to the phase-shift full-bridge PWM DC-DC converter during the half period by using the current doubler rectifier method is illustrated. If Switch S₁ is turned off in Mode 5, then it will change to Mode 6. The changes from Mode 6 to

Mode 10 are based on the changes from Mode 1 to Mode 5. The equations of the voltage and current are equal to the previous modes.

3.4 Results of Simulation and/or Considerations on the Proposed Converter

Fig. 9~12 demonstrate each simulated waveform of the high-efficiency DC-DC converter for fuel-cell systems by utilizing the modeling circuit of a fuel-cell. As shown in Fig. 9, each switch forms a zero-voltage switching. Fig. 10 demonstrates the voltage and current from the first or second side of the transformer, and the diagram shows that the low voltage(30[V]) of the fuel-cell is boosting the voltage(380[V]). Fig. 11 demonstrates the voltage and current waveforms of Diode D₅. Lastly, Fig. 12 demonstrates the current waveforms of the current output and of the inductor; it can be seen that the ripple output has been reduced.
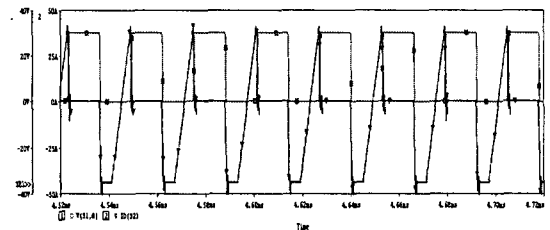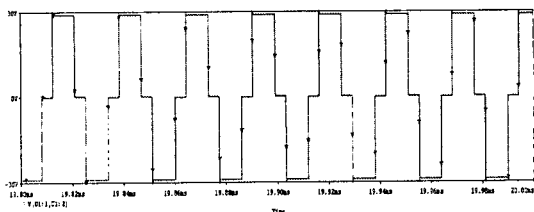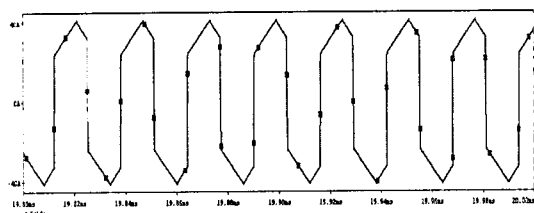

(a) Voltage and current waveforms of Switch S₂
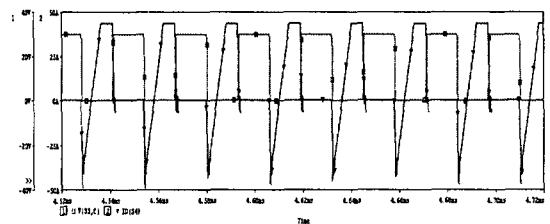
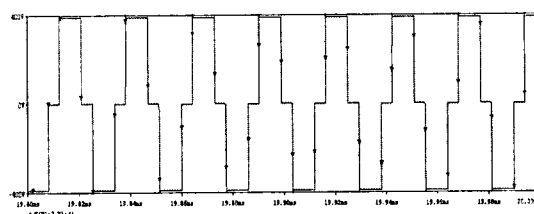(b) Voltage and current waveforms of Switch S₄

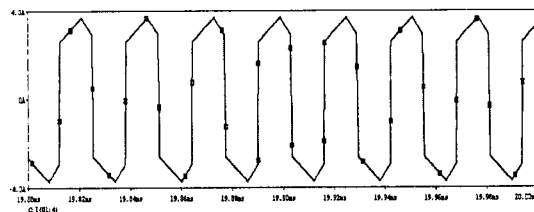**Fig. 9. Voltage and Current Waveforms of Switches**

(a) Voltage waveform from the first side
of the transformer

(b) Current waveform from the first side
of the transformer

(c) Voltage waveform from the second
side of the transformer

(d) Current waveform from the second
side of the transformer

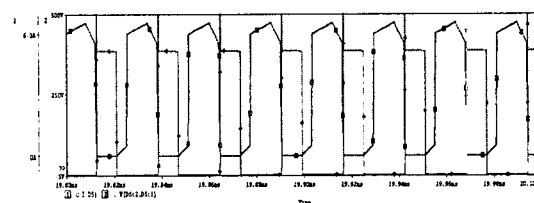**Fig. 10. Voltage and Current Waveforms of
Transformer**

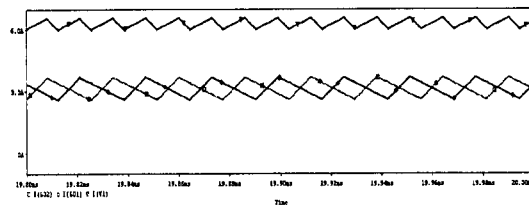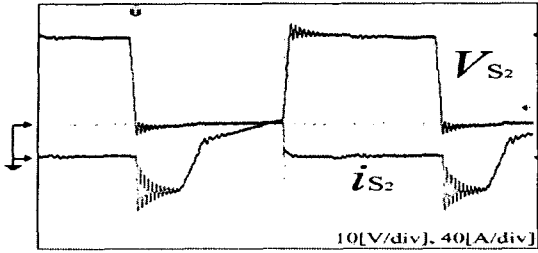**Fig. 11. Voltage and Current Waveforms of
Diode D5**

**Fig. 12. Current Waveforms of Output Current I_{out}
and Inductor Current I_{LO1}, I_{LO2}**

3.5 Results of Laboratory Experi-
ments and/or Considerations
on the Proposed Converter

Table 2 demonstrates an experimental circuit
parameter of the high-efficiency DC-DC converter
for fuel-cell systems. Figs. 13~15 demonstrate
each waveform where the duty ratio is 0.36 and
1.2[kW] for a given situation such as a properly
formed output. These diagrams are almost
equivalent to the simulated waveforms. Fig. 13
demonstrates the voltage and current waveforms,
and it was found that each switch moves to ZVS
in the diagram. Fig. 14 demonstrates the voltage
and current waveforms of the transformer, and it
shows that the voltage input(30[V]) boosts the
voltage to 400[V].

Table 2. Experimental Circuit Parameter

| Output(Pout)	1.2[kW]
Voltage input(EFC)	25~45[V]
Switching frequency(fs)	40[kHz]
Lossless snubber capacitor C_1~C4)	22[nF]
MOSFET(S1~S4; FQP65N06)	65[A], 60[V]
Diode rectifier(D5~D6; DSE120)	1200[V], 17[A]
Leakage inductance of transformer(Ll)	2[uH]
Magnetization inductance of transformer(Lm)	2.2[mH]
A ratio of a number of volumes on transformer(NP: NS)	1:16
Output inductor(L01(=L02))	2.8[mH]
Output capacitor(C0)	2200[uF]

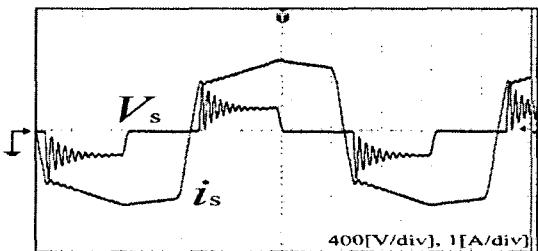(a) Voltage and current waveforms of
Switch S_2
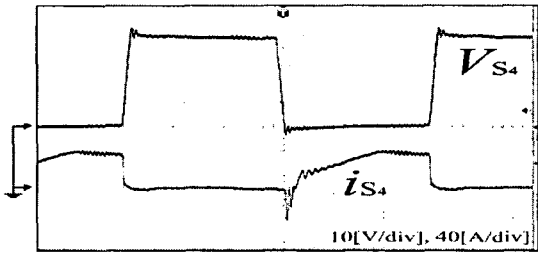
(b) Voltage and current waveforms of
Switch S_4

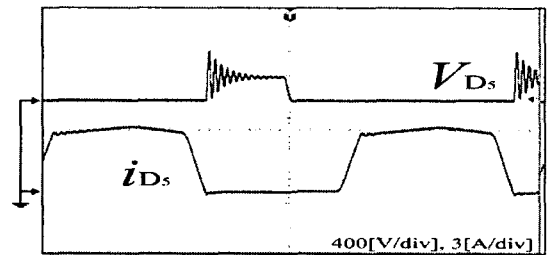**Fig. 13. Voltage and Current Waveforms of
Switches**
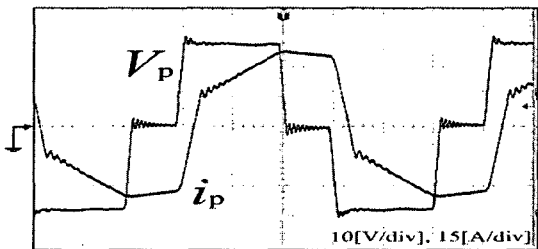
(a) Voltage and current waveforms from
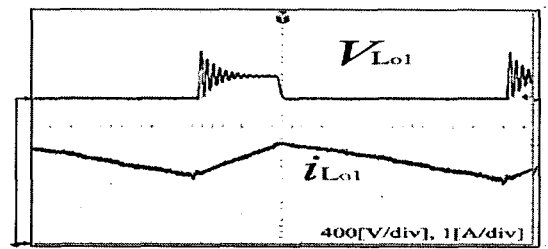the first side of the transformer

(b) Voltage and current waveforms from
the second side of the transformer

**Fig. 14. Voltage and Current Waveforms of
Transformer**

Fig. 15 demonstrates the voltage and current waveforms of the rectifier, where the amount of Diode D_5 is electrically attained during the half period. The diagram also shows that the current ripple is reduced by the voltage and the current waveforms through the inductor L_{01}. Figs. 16 and 17 demonstrate each waveform in a situation like the highest duty ratio(D_{MAX}=0.4). In the diagrams, the switch moves to ZVS when the duty ratio(0.4) is the highest.
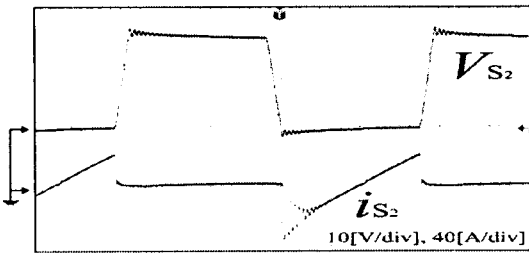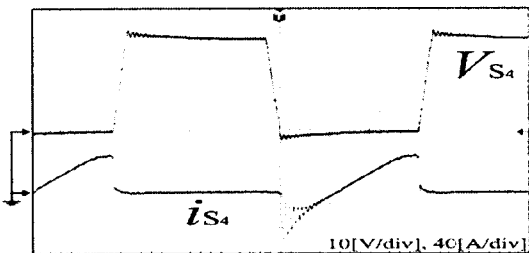
(a) Voltage and current waveforms of
Diode D_5

(b) Voltage and current waveforms of
inductor L_{01}

**Fig. 15. Voltage and Current Waveforms of
Rectifier**

Figure 18 demonstrates the efficiency and the current output. As the diagram shows, the highest efficiency is 92[%].
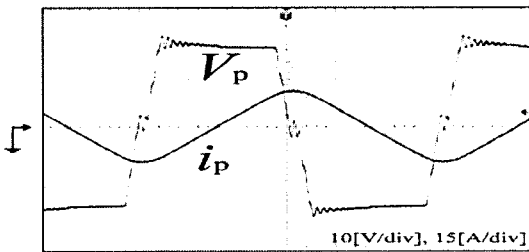
Soon-Kurl Kwon

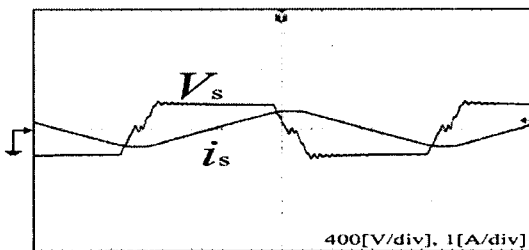(a) Voltage and current waveforms of Switch S₂

(b) Voltage and current waveforms of Switch S₄

Fig. 16. Voltage and Current Waveforms of Switches(The State of Duty Ratio Maximum)

(a) Voltage and current waveforms from the first side of the transformer

(b) Voltage and current waveforms from the second side of the transformer

Fig. 17. Voltage and Current Waveforms of Transformer(The State of Duty Ratio Maximum)
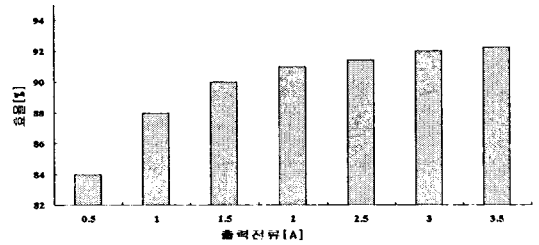

Fig. 18. Efficiency characteristics for output current

4. Conclusion

By utilizing the Nexa(310-0027) PEMFC from the Ballard Co., this study proposes a high-efficiency DC-DC converter for fuel-cell systems. The main purpose was to boost the low voltage output by using a new current doubler rectifier method. Three major results are listed below:

(1) The proposed high-efficiency DC-DC converter used the phase-shift PWM control method and accomplished ZVS by partial resonance. Thus, the proposed converter reduced the constant switching frequency, the loss of switching of the switch, and the peak voltage and current.

(2) By adding two inductors to the rectifier circuit, it was able to supply the DC voltage and current of the reduced ripple safely to the load.

(3) By utilizing the newly proposed current doubler rectifier, the high-efficiency DC-DC converter for fuel-cell systems reached the highest efficiency(92[%]). As compared to the previous converter, the rate of efficiency was increased by 3.7[%].

Based on the results of the proposed electric-power converter for fuel-cells, the utilization of industrial use fuel-cells, domestic gas services, motor vehicles, and electric appliances will benefit from the design of the electric-power converter.

71

References

[1] Andrew Dicks, "Fuel Cell Handbook, sixth Edition" EG & G Technical Services Inc., May 2002.

[2] J. E. Larminie and A. Dicks, "Fuel Cell Systems Explained. Chichester",U.K.: Wiley, 2000, p. 308.

[3] S. K. Mazumder, and R. S. Gemmen, "Solid- Oxide-Fuel-Cell Performance and Durability: Resolution of the Effects of Power Conditioning Systems and Application Loads", IEEE Trans. On Power Electronics, Vol.19, No.5, 2004.

[4] R. J. Wai and R. Y. Duan, "High-Efficiency Power Conversation for Low Power Fuel cell Generation System", IEEE Trans. On Power Electronics, Vol.20, No.4, pp.847~856, 2005.

[5] T.W.Lee, S.H.Kim, C.Y.Won, "Development of A 3[kW] Fuel Cell Generation System with An Active Fuel Cell Simulator: Topology, Control, and Design", Conf. Rec. of IEEE PESC, pp.4743~4748, 2004.

[6] T.W.Lee, S.J.Jang, H.K.Jang and C.Y.Won, "A Fuel Cell Generation System With a Fuel Cell Simulator" JOURNAL OF POWER ELECTRONICS, Vol.5, No.1, pp.55~61. 2005.

[7] S. H, LEE S. K. KWON, H. W. LEE, "A Circuit Model of PEMFC for Design and Analyze Fuel Cell Power System" Power Electronics Summer Conference, pp.197~199, 2006.

[8] S. H, LEE S. K. KWON, K. Y. Suh, J. Y. KIM, "Topology of the Novel High Frequency Insulated Soft Switching PWM DC-DC Converter" KIIEE Journal Vol.20, No.1, pp.119~124, 2006.

[9] T.W. Lee, S.J.Jang, J.T.Kim, J.S.Gu, C.Y.Won, C.H. Kim "A Study on PWM Converter/Inverter Drive System by a Fuel Cell Simulator", KIPE Journal, Vol. 9, No. 3, pp.222~230, 2004.

[10] Patterson and D. M. Divan, "Pseudo-resonant full bridge DC/DC converter", IEEE PESC Record, Vol. 2, pp. 424~430, 1987.

[11] S.J. Jeon, G. H. Cho, "A zero-voltage and zero-current switching full bridge DC-DC converter with transformer isolation", IEEE Trans., Vol. 16, No. 5, pp. 573~580, 2001.

[12] K. W. Seok, B. H. Kwon, "An improved zero-voltage and zero current switching full-Bridge PWM converter using a simple resonant circuit", IEEE Trans. on Ind. Electronics, Vol. 48, No. 6, pp. 1205~1209, 2001.

Biography

Soon-Kurl Kwon

He received a Ph. D(Dr-Eng) degree in Electrical Engineering from Young-Nam University, Daegu, Republic of Korea. He joined the Electrical Engineering Department of Kyungnam University, Masan, Republic of Korea in 1983 and has served as a professor. He was a visiting professor of VPEC in VPI & SU, UAS in 1997. His research interests include application developments of power electronics circuits and system. He is a member of the KIEE, KIPE, KIIEE, and IEEE.